

Supporting Information

Electronic and molecular structure relations in diiron compounds mimicking the [FeFe]-hydrogenase active site studied by X-ray spectroscopy and quantum chemistry

Ramona Kositzki¹, Stefan Mebs¹, Nils Schuth¹, Nils Leidel¹, Lennart Schwartz², Michael Karnahl^{2,3}, Florian Wittkamp⁴, Daniel Daunke⁵, Andreas Grohmann⁵, Ulf-Peter Apfel⁴, Frédéric Gloaguen⁶, Sascha Ott², and Michael Haumann^{1*}

¹Freie Universität Berlin, Fachbereich Physik, 14195 Berlin, Germany

²University of Uppsala, Department of Chemistry, Ångström Laboratories, 75120 Uppsala, Sweden

³present address: University of Stuttgart, Institute of Organic Chemistry, 70569 Stuttgart, Germany

⁴Ruhr-Universität Bochum, Anorganische Chemie I, 44801 Bochum, Germany

⁵Technische Universität Berlin, Institut für Chemie, Bioanorganische Chemie, 10623 Berlin, Germany

⁶CNRS, Université de Bretagne Occidentale, UMR 6521, 29238 Brest, France

Table S1: Bond lengths in diiron compounds.^a

compound	mean bond length [Å]				
	Fe-Fe distance	Fe-ligand distance	terminal CO ligands	other terminal ligands	bridging ligands
1	2.539 (2.541)	2.032 (2.046)	1.763 (1.746)	2.128 (2.155)	1.925 (1.922)
2	2.556 (2.578)	1.972 (1.979)	1.796 (1.782)	-	2.234 (2.275)
3	2.510 (2.543)	1.981 (1.990)	1.800 (1.786)	-	2.252 (2.295)
4	2.494 (2.530)	1.985 (1.992)	1.800 (1.786)	-	2.263 (2.301)
5	2.480 (2.513)	1.982 (1.995)	1.792 (1.786)	-	2.268 (2.307)
6	2.512 (2.535)	1.988 (1.996)	1.799 (1.791)	-	2.272 (2.304)
7	2.508 (2.535)	1.826 (1.851)	1.768 (1.791)	-	1.914 (1.940)
8	2.555 (2.622)	2.051 (2.071)	1.758 (1.758)	2.237 (2.272)	2.252 (2.285)
9	2.569 (2.599)	2.047 (2.074)	1.755 (1.754)	2.222 (2.271)	2.252 (2.295)
10	2.546 (2.583)	2.050 (2.071)	1.758 (1.758)	2.221 (2.252)	2.256 (2.294)
11	2.552 (2.569)	2.002 (2.010)	1.790 (1.774)	2.064 (2.081)	2.251 (2.288)
12	2.519 (2.546)	2.017 (2.027)	1.787 (1.776)	2.203 (2.222)	2.258 (2.292)
13	2.531 (2.571)	2.073 (2.081)	1.779 (1.772)	2.217 (2.243)	2.296 (2.308)
14	2.544 (2.595)	2.059 (2.078)	1.781 (1.775)	2.206 (2.245)	2.263 (2.299)
15	2.497 (2.559)	2.061 (2.082)	1.771 (1.775)	2.197 (2.230)	2.284 (2.314)
16	2.518 (2.582)	1.991 (2.008)	1.737 (1.754)	1.926 (1.913)	2.276 (2.309)
17	2.509 (2.563)	2.000 (2.010)	1.746 (1.750)	1.942 (1.916)	2.283 (2.316)
18	2.518 (2.584)	1.991 (2.007)	1.737 (1.754)	1.926 (1.912)	2.276 (2.308)

^aBond lengths refer to crystal structures or to geometry-optimized structures (BP86/TZVP, COSMO solvation model, $\epsilon = 4$; in parenthesis).

Table S2: K-edge and $K\beta_{1,3}$ line energies.^a

compound	E(K_{edge}) [eV]	E($K\beta_{1,3}$) [eV]
1	7123.2	7057.09
2	7123.2	7057.08
3	7123.9	7057.05
4	7123.8	7057.06
5	7124.4	7057.02
6	7124.6	7057.10
7	7125.1	7057.00
8	7122.6	7057.20
9	7122.6	7057.23
10	7121.8	7057.24
11	7122.7	7057.20
12	7122.2	7057.10
13	7121.0	7057.10
14	7120.4	7057.11
15	7120.3	7057.12
16	7123.4	7056.98
17	7123.1	7056.96
18	7123.4	7057.00

^aData correspond to spectra in Fig. 3A,B and to data in the insets. The K-edge energy (at 50 % level) error is ~ 0.1 eV, the $K\beta_{1,3}$ line energy error from 1st-moment calculation is ~ 0.05 eV.

Table S3: Fit parameters for calculated vs. experimental ctv and vtc energies and intensities.^a

spectra	peak	energy			intensity		
		offset [eV]	slope	R	offset [r.u.]	slope	R
ctv	1	1452	0.80	0.61	0.05	0.45	0.56
	2	2697	0.63	0.68	0.02	0.22	0.39
vtc	1	4901	0.31	0.37	-0.01	0.45	0.70
	2	5069	0.29	0.31	0.05	-0.17	0.44
	3	4211	0.41	0.64	0.03	0.93	0.73
	4	4363	0.39	0.74	0.02	0.71	0.71
	5	4964	0.30	0.74	0.06	0.44	0.84
	6	2619	0.63	0.70	0.02	0.61	0.83

^aValues correspond to linear fits ($E/I_{\text{cal}} = \text{offset} + \text{slope} \times E/I_{\text{exp}}$) of plots of DFT-calculated vs. experimental (Figs. 4 and 5) data points for energies and intensities of individual ctv and vtc peaks in Fig. 6. Note R-values (shaded).

Table S4: Normalized iron parameters.^a

observable	compound															
	2	3	5	4	6	8	11	9	10	12	14	13	15	18	16	17
	normalized parameter															
Fe-Fe distance	89	33	0	11	33	78	78	100	78	44	67	56	22	44	44	33
Fe charge	100	82	83	80	78	9	86	14	8	43	2	0	2	11	13	6
HOMO energy	95	75	86	76	100	25	47	24	24	50	58	60	67	0	5	5
vtc energy	89	81	79	100	86	93	36	44	46	69	51	88	46	41	36	0
K $\beta_{1,3}$ energy	43	32	21	36	25	86	76	96	100	79	54	50	57	14	7	0
LUMO energy	100	85	91	84	90	30	42	22	22	46	44	30	44	0	5	14
ctv energy	47	100	92	35	26	93	13	51	78	21	70	19	29	7	0	3
K-edge energy	67	84	94	82	100	54	56	53	35	45	2	17	0	61	62	56
Fed degeneracy	100	24	64	31	39	50	31	35	47	29	27	0	17	39	39	67
Fed localization	80	75	46	76	14	64	100	63	27	30	0	17	12	47	44	32
mean	81	67	66	61	59	58	57	50	47	46	37	34	30	27	26	22

^aNormalized parameter values (P^{norm} , rounded to integer values) for each observable (O) and compound (i) were calculated according to (O^{min} and O^{max} = minimal or maximal observable values in the series of compounds): $P_i^{\text{norm}} = (O_i - O^{\text{min}}) / (O^{\text{max}} - O^{\text{min}}) \times 100$.

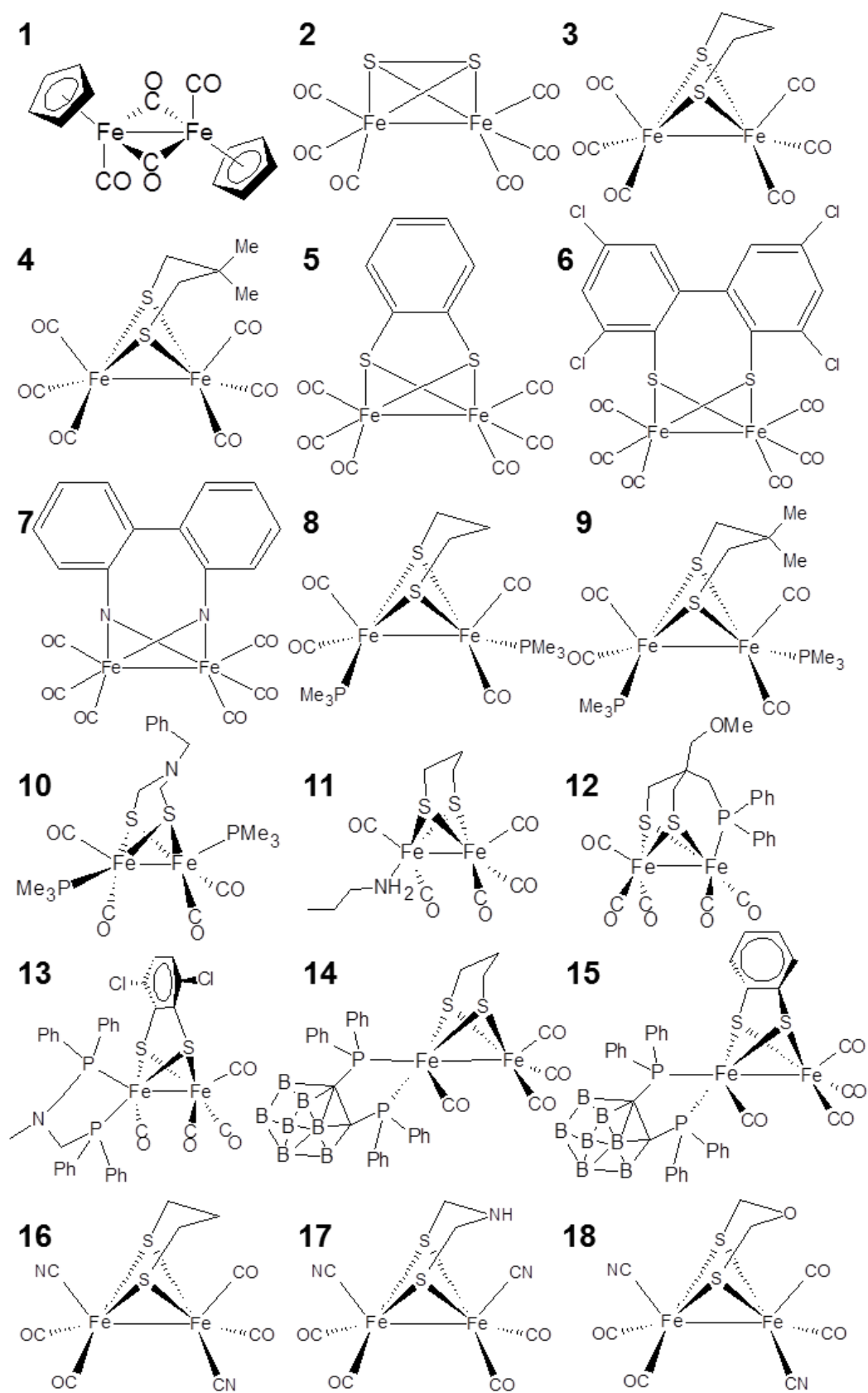


Figure S1: Schematic drawing of the structures of the diiron compounds. For crystal structures see Fig. 2.

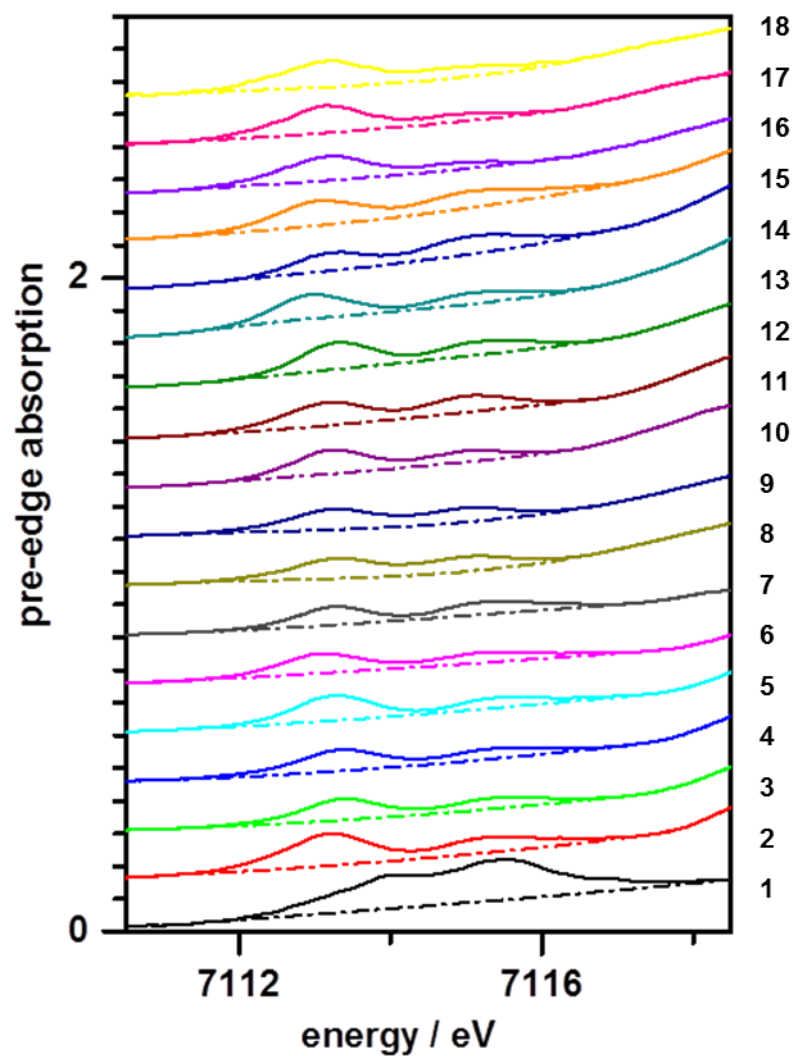


Figure S2: Pre-edge absorption features in the XANES. Spectra correspond to data of the 18 compounds in Fig. 3A with the pre-edge absorption region shown in magnification (spectra vertically shifted for comparison). Subtraction of smooth background curves (dash-dotted lines) from the spectra yielded the experimental ctv spectra shown in Fig. 4A.

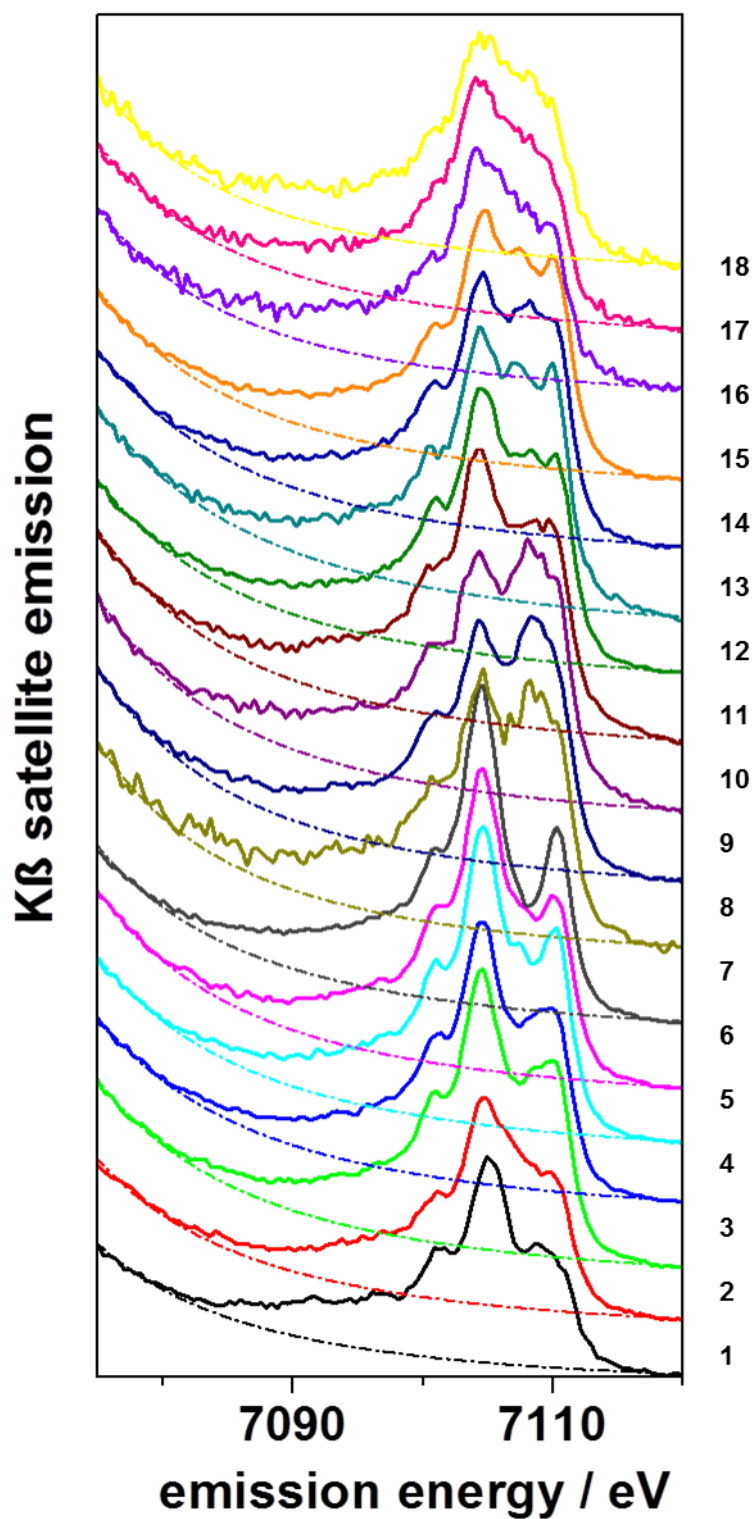


Figure S3: Experimental $K\beta$ satellite emission spectra. Non-normalized spectra in the $K\beta$ satellite emission region of the 18 compounds indicated on the right were vertically shifted for comparison. Subtraction of background curves (dash-dotted lines) and normalization of the resulting spectra to unity area yielded the experimental vtc spectra shown in Fig. 5A.

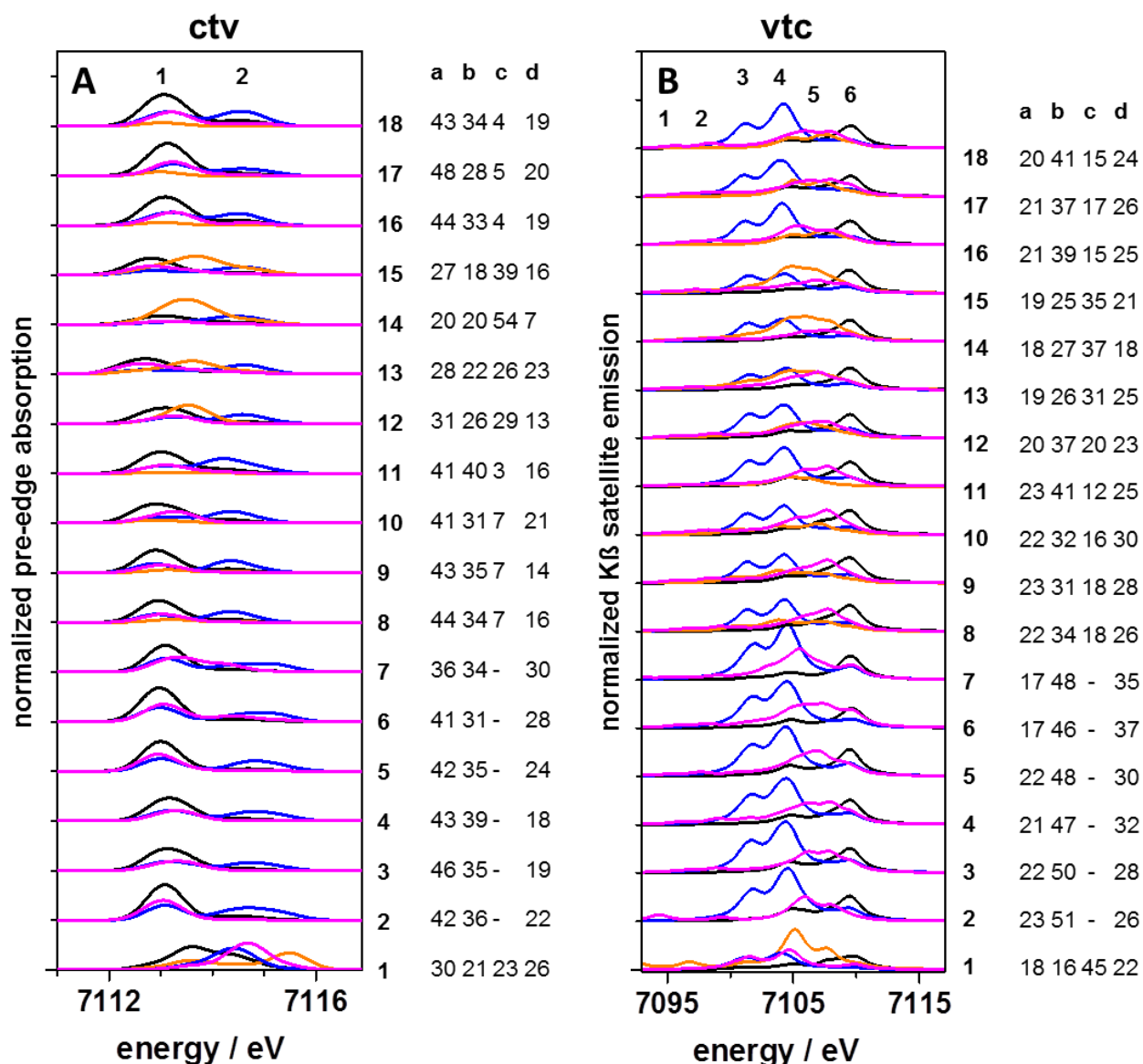


Figure S4: Iron and ligand contributions to ctv and vtc spectra from DFT. (A) Characters of target MOs for ctv electronic excitation transitions in Fig. 4B. (B) Characters of target MOs for vtc electronic decay transitions in Fig. 5B. Color code in A and B: Fe, black; terminal CO ligands, blue; other terminal ligands, orange; bridging ligands, magenta. Numbers on the right in (A) and (B) denote: 1st column, diiron compound; and 2nd to 5th column (a, b, c, d), rounded contribution of the spectra of Fe, terminal CO ligands, other terminal ligands, and bridging ligands to the envelope spectrum (see Figs. 4 and 5) in percent. Spectra were vertically shifted for comparison. Numbers above the top spectrum in (A) and (B) correspond to discernable peak features (2 in ctv and 6 in vtc spectra) in the envelope spectra.

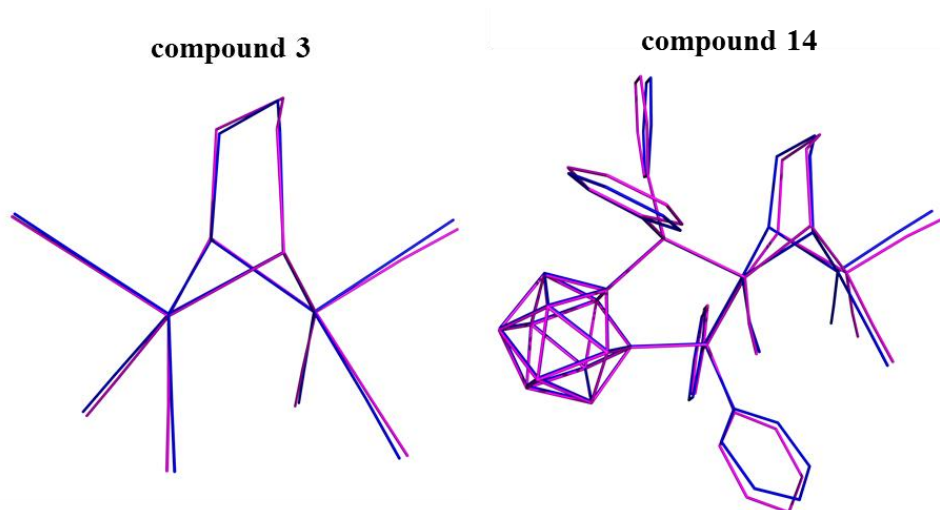


Figure S5: Crystal structures and geometry-optimized structures. Colours: blue lines = crystal structures; magenta lines, geometry-optimized structures (Table S1). Protons were omitted for clarity. Note small coordinate deviations between crystal and relaxed structures for the symmetric (**3**) and asymmetric (**14**) compounds, which were also found for the remaining compounds (Table S1, Fig. S6). Relaxed structures were only used for calculation of CM5 charges (Fig. 9) whereas crystal structures were used for calculation of ctv/vtc spectra (Figs. 4-8) and electronic parameters (Figs. 10 and 11, Table 2).

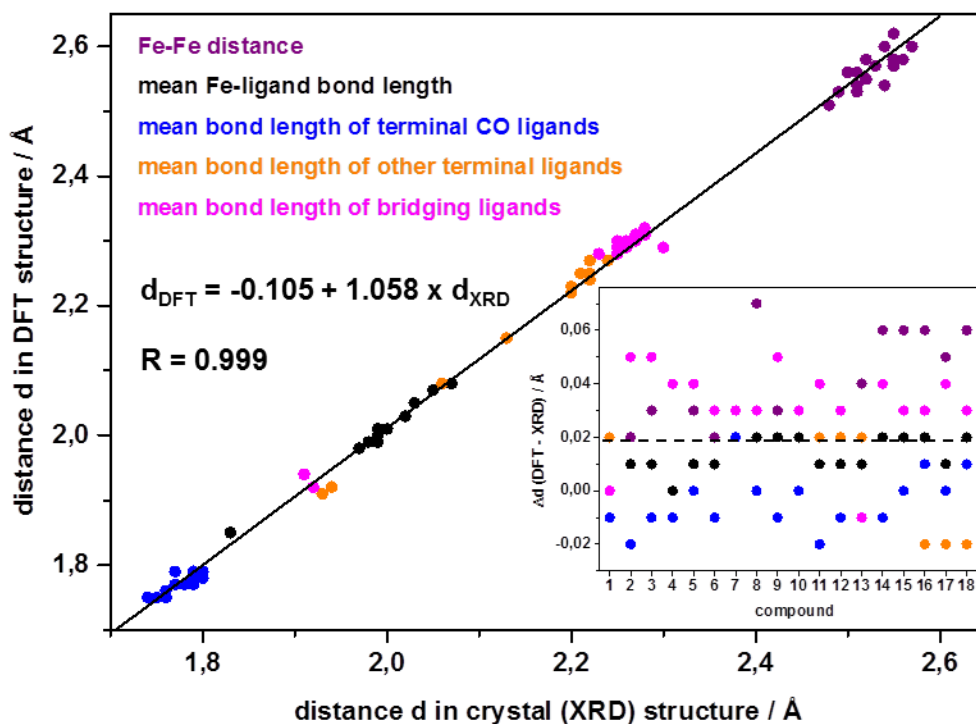


Figure S6: Interatomic distances in **1-18** from crystal and relaxed structures. For individual bond lengths in the compounds in crystal structures and geometry-optimized structures from DFT see Table S1. Note good correlation of distances in DFT and XRD structures and overall small overestimation of distances (mean of ~ 0.02 Å, inset) by the DFT approach.

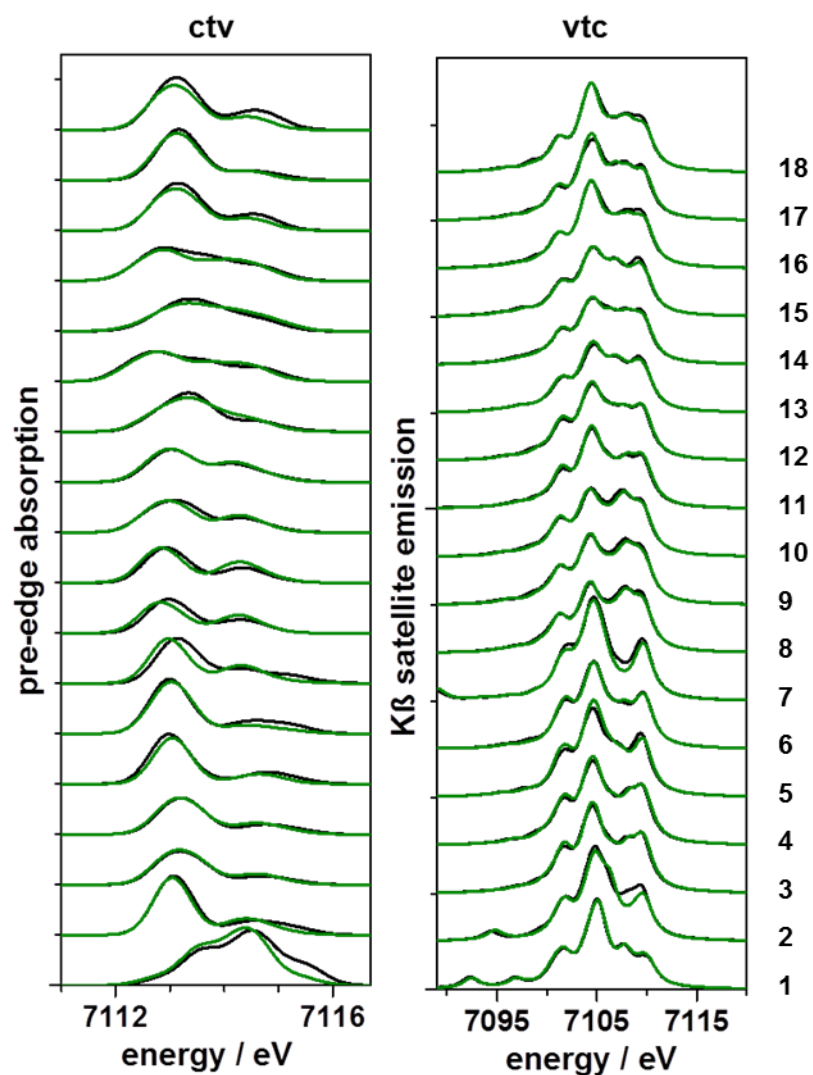


Figure S7: Calculated ctv and vtc spectra for crystal and relaxed structures. Left: ctv spectra. Right: vtc spectra. Black lines, spectra from single-point DFT calculations on crystal structures; green lines, calculations on DFT geometry-optimized structures (Table S1) for compounds indicated on the right. Note high similarity of ctv/vtc spectra from both computational approaches.

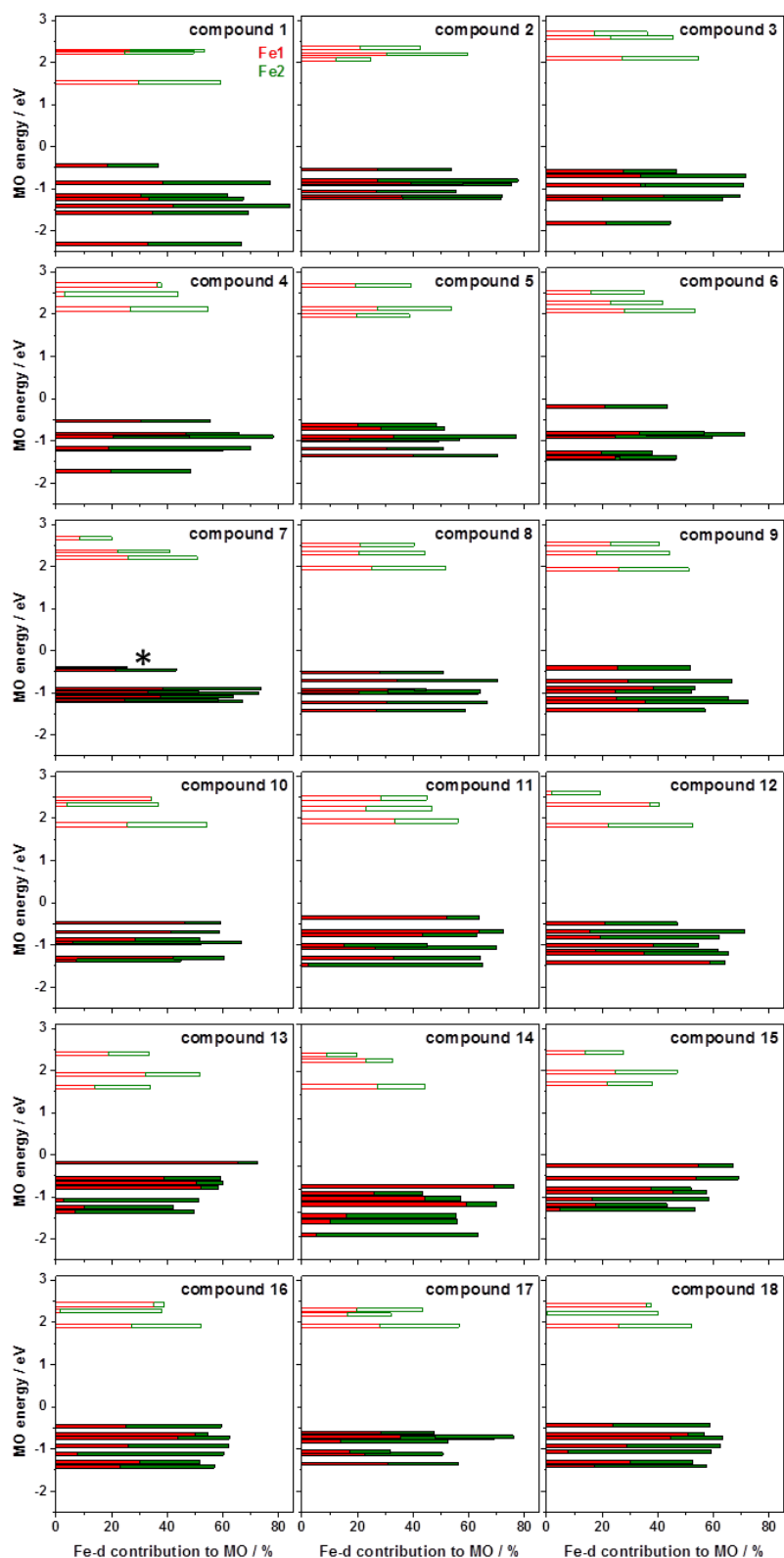


Figure S8: Fe(d) character and energy of valence MOs. Bars show the Fe(d) character contribution of Fe1 (red) and Fe2 (green) to the 10 valence MOs (open bars, unoccupied MOs; solid bars, double occupied MOs; *the black solid bar for 7 shows the HOMO). The mean energy of the MOs for each compound was set to zero.

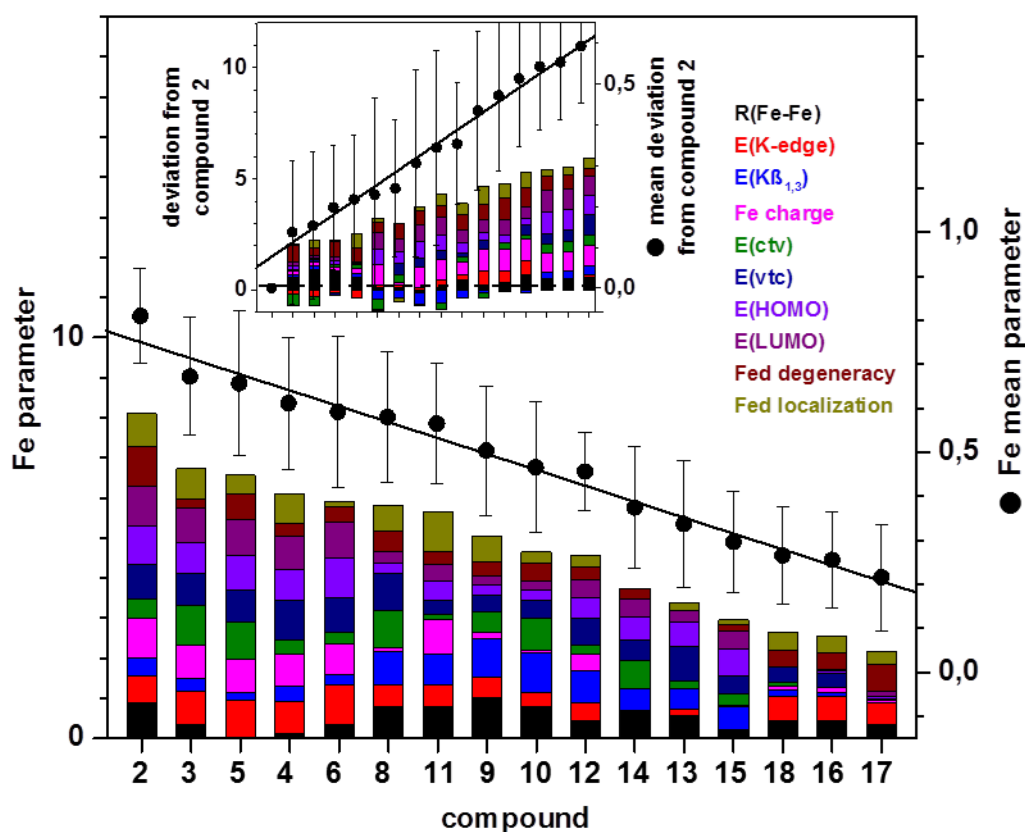


Figure S9: Relation of normalized structural and electronic parameters. For the 16 compounds with a dithiolate bridge, the ranges of the experimental and calculated parameters related to the properties of iron, i.e. the Fe-Fe distance and Fe charge, energy of valence levels (occupied MOs: HOMO, vtc, and $K\beta_{1,3}$ energies; unoccupied MOs: LUMO, ctv, and K-edge energies), and Fe(d) level degeneracy and localization, were normalized between 0-1 (Table S4) and normalized values were averaged so that a mean apparent Fe parameter was derived. Main panel: indicated individual normalized parameters (coloured bars, left y-axis) and mean Fe parameter ($\sum p_i^{\text{norm}}/10$, solid circles, right y-axis). Inset: deviations of individual parameters for compounds 3-18 from the respective values of compound 2 (coloured bars, left y-axis) and mean Fe parameter deviations (solid circles, right y-axis). Error bars show standard deviations, regression lines guide the eye, ctv and vtc energies correspond to mean energies of 2 or 6 peak features in the experimental spectra (Figs. 4A and 5A), Fe(d) degeneracy and localization refers to the mean energy ranges of, or to the mean Fe(d) contribution to unoccupied and occupied MOs (Table 2). Note the ordering of compounds on the x-axis.

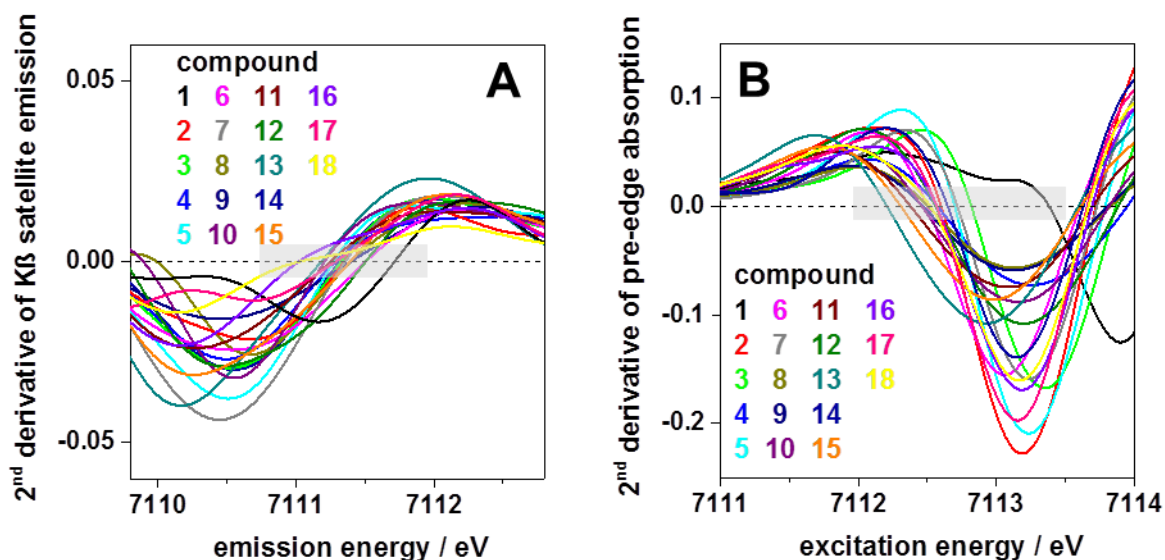


Figure S10: Second derivative spectra of experimental vtc and ctv spectra of **1-18**. (A) K $\beta_{2,5}$ emission spectra (vtc). (B) Pre-edge absorption spectra (ctv). Apparent relative HOMO or LUMO energies and respective energy gaps were derived from the spectra by determination of the zero crossing point at highest (vtc) or lowest (ctv) energy (marked by the dashed line and grey-shaded rectangle in A and B). The vtc and ctv spectra (Figs. S2 and S3) were smoothed by adjacent averaging over 3 data points and 1st and 2nd derivative spectra were calculated using cubic spline smoothing over 10 (vtc) or 5 (ctv) data points to yield the shown spectra.